

CHEMISTRY

A European Journal

A Journal of



Accepted Article

Title: Design of Na⁺-Selective Fluorescent Probes - A Systematic Study of the Na⁺-Complex Stability and the Na⁺/K⁺ Selectivity in Acetonitrile and Water

Authors: Hans-Jürgen Holdt

This manuscript has been accepted after peer review and appears as an Accepted Article online prior to editing, proofing, and formal publication of the final Version of Record (VoR). This work is currently citable by using the Digital Object Identifier (DOI) given below. The VoR will be published online in Early View as soon as possible and may be different to this Accepted Article as a result of editing. Readers should obtain the VoR from the journal website shown below when it is published to ensure accuracy of information. The authors are responsible for the content of this Accepted Article.

To be cited as: *Chem. Eur. J.* 10.1002/chem.201605986

Link to VoR: <http://dx.doi.org/10.1002/chem.201605986>

Supported by
ACES

WILEY-VCH

Design of Na⁺-Selective Fluorescent Probes – A Systematic Study of the Na⁺-Complex Stability and the Na⁺/K⁺ Selectivity in Acetonitrile and Water

Thomas Schwarze,^[a] Holger Müller,^[a] Darya Schmidt,^[a] Janine Riemer^[a] and Hans-Jürgen Holdt^{*[a]}

Abstract: Overall, there is a tremendous demand for highly Na⁺-selective fluoroionophores to monitor the top analyte Na⁺ in life science. Herein, we report on a systematic route to develop highly Na⁺/K⁺ selective fluorescent probes. Thus, we synthesized a set of fluoroionophores **1**, **3**, **4**, **5**, **8** and **9** (cf. Scheme 1) to investigate the Na⁺/K⁺ selectivity and Na⁺-complex stability in CH₃CN and H₂O. These Na⁺-probes bearing different 15-crown-5 moieties to bind Na⁺ stronger than K⁺. In the set of the diethylaminocoumarin substituted fluoroionophores **1-5** following trend of the fluorescence quenching **1** > **3** > **2** > **4** > **5** in CH₃CN (cf. Table1) was observed. Therefore, the flexibility of the aza-15-crown-5 moieties in **1-4** determines the conjugation of the nitrogen lone pair with the aromatic ring. As a consequence, **1** showed in CH₃CN the highest Na⁺ induced fluorescence enhancement (FE) by a factor of 46.5 and a weaker K⁺ induced FE of 3.7. The Na⁺-complex stability of **1-4** in CH₃CN is enhanced in the following order **2** > **4** > **3** > **1**, assuming that the O-atom of the methoxy group in ortho position, as shown in **2**, strengthened the Na⁺-complex formation. Further, we found for the *N*-(*o*-methoxyphenyl)aza-15-crown-5 substituted fluoroionophores **2**, **8** and **9** in H₂O an enhanced Na⁺-complex stability in the following order **8** > **2** > **9** and an increased Na⁺/K⁺ selectivity in the reverse order **9** > **2** > **8**. Notable, the Na⁺ induced FE of **8** (FEF = 10.9), **2** (FEF = 5.0) and **9** (FEF = 2.0) showed a similar trend associated with a decreased K⁺ induced FE (**8** (FEF = 2.7) > **2** (FEF = 1.5) > **9** (FEF = 1.1)). Herein, the Na⁺-complex stability and Na⁺/K⁺ selectivity is also influenced by the fluorophore moiety. Thus, fluorescent probe **8** (K_d = 48 mM) allows high-contrast, sensitive and selective Na⁺ measurements over extracellular K⁺ levels. A higher Na⁺/K⁺ selectivity showed fluorescent probe **9**, but also a higher K_d value of 223 mM. Therefore, **9** is a suitable tool to measure Na⁺ concentrations up to 300 mM at a fluorescence emission of 614 nm.

Introduction

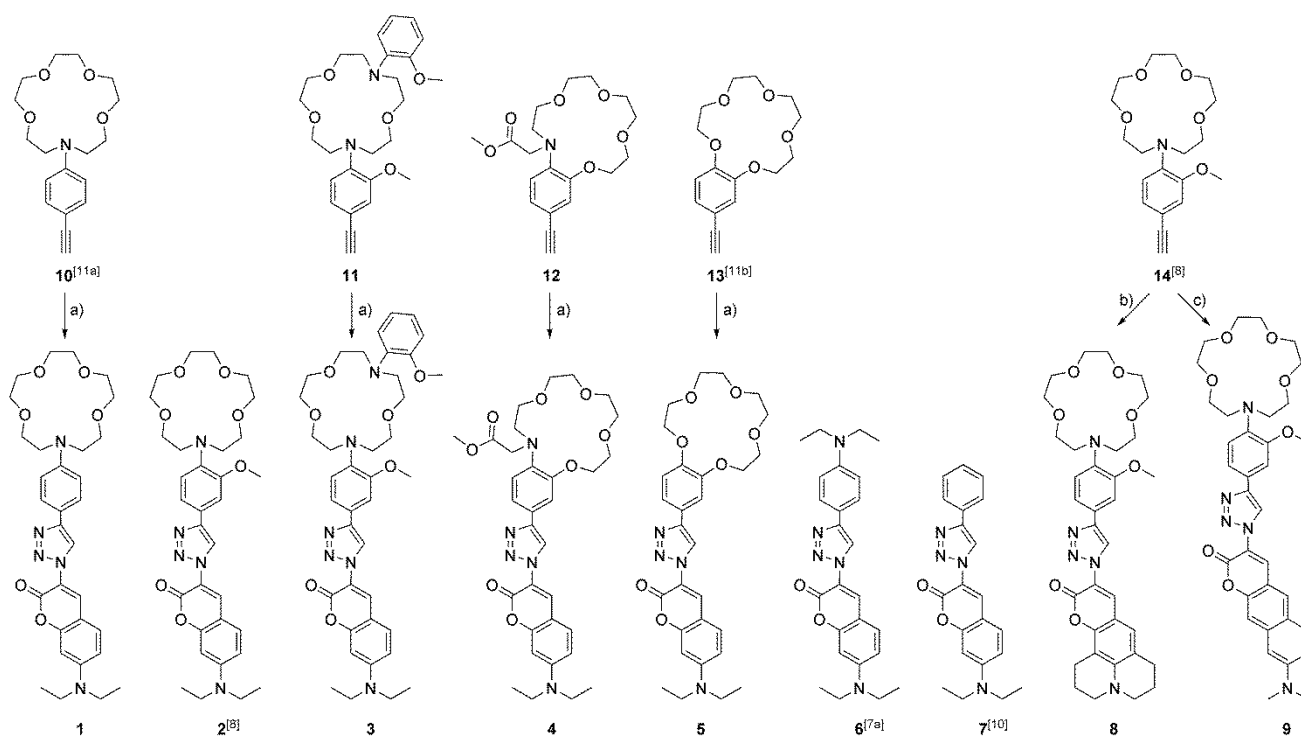
Sodium is one of the most important analytes in life science. It plays a vital role by diverse physiological and pathological processes, such as nerve conduction and muscle and heart

contraction.^[1a,b] In animal cells the Na⁺ concentration range differs in the intra- (5-30 mM) and extracellular (100-150 mM) space.^[2] In both, K⁺ is the competitive cation and shows an extra-(1-10 mM) and intracellular (100-150 mM) concentration gradient contrary to Na⁺. Hence, for a reliable Na⁺ analyses in vivo highly Na⁺/K⁺ selective tools were required. A favored strategy to determine Na⁺ in vitro and in vivo is based on the highly sensitive fluorescence spectroscopy method. The non-fluorescent Na⁺ is detected by fluorescent probes, which containing an ion-binding moiety (ionophore) and a fluorescence sensing unit (fluorophore). These fluorescent probes, so-called fluoroionophores, show Na⁺-dependent fluorescence intensity changes. Minta and Tsien designed the first fluoroionophore SBFI (short for sodium-binding benzofuran isophthalate) for intracellular Na⁺ levels (5-30 mM).^[2] SBFI contains of a *N,N*-bis(*o*-methoxyphenyl)diaza-15-crown-5 moiety, which is the most commonly used ionophore to detect intracellular Na⁺ levels. Up to now, various fluoroionophores for a determination of intracellular Na⁺ levels were reported.^[3a-e] Nowadays, the authors focused on the spectroscopic properties of the fluorophore moiety.^[3c-e] There, ratiometric red-fluorescent^[3e] and two photon excitable^[3c,d] Na⁺-fluoroionophores were developed. Further, to determine extracellular Na⁺ levels (100-140 mM), He et al.^[4a] and Gunnlaugsson et al.^[4b] designed fluoroionophores based on a *N*-(*o*-methoxyphenyl)aza-15-crown-5 ionophore. For the detection of higher Na⁺ levels >140 mM, a few fluoroionophores were available.^[5a-c] They contain as an ionophore a *N*-methylacetate-aza-15-benzo-crown-5^[5a] or a *N*-phenylaza-15-crown-5^[5c] moiety. A further Na⁺-selective binding moiety is the nitrogen-free benzo-15-crown-5 ionophore, which is part of Na⁺-fluoroionophores^[6a,b], for instance, to determine Na⁺ near micelle surfaces.^[6b]

All in all, there is rare number of fluoroionophores for a Na⁺ determination in vitro or in vivo. Therefore, tailor-made and easily accessible Na⁺-fluoroionophores with a high Na⁺/K⁺ selectivity and with an appropriate dissociation constant to detect Na⁺ in vitro and in vivo should be further developed.

[a] Dr. T. Schwarze, H. Müller, D. Schmidt, J. Riemer, Prof. Dr. H.-J. Holdt
Institut für Chemie, Anorganische Chemie, Universität Potsdam
Karl-Liebknecht-Str. 24–25, 14476 Golm (Germany)
E-mail: holdt@uni-potsdam.de

Supporting information for this article is given via a link at the end of the document.



Scheme 1. Synthesis of Na⁺-responsive fluoroionophores **1**, **3**, **4**, **5**, **8** and **9**: a) CuSO₄/Na ascorbate, 3-azido-7-diethylaminocoumarin^[10], THF/H₂O, 60°C; b) CuSO₄/Na ascorbate, 10-azido-2,3,6,7-tetrahydro-1*H*,5*H*,11*H*-[1]benzopyrano[6,7,8-*ij*]quinolizin-11-one^[10], THF/H₂O, 60°C; c) CuSO₄/Na ascorbate, 3-azido-8-(dimethylamino)-2*H*-benzo[*g*]chromen-2-one^[13], THF/H₂O, 60°C.

Recently, we found that in CuAAC (short for Cu(I)-catalyzed 1,3-dipolar azide alkyne cycloaddition reaction) generated fluoroionophores, the electronic conjugation of a *N*-phenylaza-18-crown-6 and a 7-diethylaminocoumarin fluorophore through a 1,2,3-triazol-1,4-diyl π -linker results in a perfect signal transduction chain for the sensing of K⁺ under simulated physiological conditions, but not for physiological relevant K⁺ levels.^[7a] Further, we attached in ortho position of the aniline unit different alkoxy groups to enhance the K⁺ complex stability and the K⁺/Na⁺ selectivity.^[7b-d] In addition, we successfully transferred the signal transduction chain to an exclusive Na⁺ sensing by introduction of a *N*-(*o*-methoxyphenyl)aza-15-crown-5 ionophore as shown in fluoroionophore **2** (Scheme 1).^[8] Fluorescent probe **2** showed a high Na⁺/K⁺ selectivity when embedded in a polymethacrylate hydrogel and a moderate Na⁺/K⁺ selectivity under simulated physiological conditions.^[8] There, we reached a better Na⁺/K⁺ selectivity and a higher Na⁺-induced fluorescence enhancement (FE), when the aniline donor is connected to the position 4 of the triazole and the coumarin acceptor to the position 1, as shown in fluorescent probe **2** (cf. Scheme 1).

Herein, our superior goal is to synthesize easily accessible and highly Na⁺/K⁺ selective fluorescent probes, which based on a electron withdrawing 1,2,3-triazole unit to benefit of a selectivity advantage, as already shown for the highly K⁺/Na⁺ selective fluorescent probes^[7a-d].

Results and Discussion

To study the Na⁺/K⁺ selectivity and the Na⁺-complex stability in combination with the above-mentioned signal-transduction-chain: anilino-triazole-coumarin, we introduced different 15-membered crown ether derivatives as Na⁺-ionophores, which are promising candidates for an exclusively binding of Na⁺ over K⁺. Further, to investigate influences of flexibilities of aza-15-crown-5 ionophores towards the fluorescence quenching in these fluoroionophores and therefore for an effective sensing of Na⁺ in CH₃CN and in H₂O, we synthesized fluorescent probes **1**, **3**, **4**, **8** and **9**. These fluorescent probes consisting of different 15-membered crown ionophores (cf. Scheme 1). The *N*-phenylaza-15-crown-5 ionophore was introduced in **1**. Fluorescent probes **2**, **8**, and **9** containing of a *N*-(*o*-methoxyphenyl)aza-15-crown-5 ionophore. Further, **3** based on a *N,N*-bis(*o*-methoxyphenyl)diaza-15-crown-5 ionophore and **4** on a *N*-methylacetate-aza-15-benzo-crown-5 ionophore. For comparison, we synthesized fluorescent probe **5** with a benzo-15-crown-5, as the Na⁺-recognition unit. Further, to maintain the above-mentioned signal transduction chain, we selected as fluorophores, coumarin or π -extended coumarin derivatives with different fluorescence maxima λ_{\max} and fluorescence quantum yields ϕ_f in polar solvents. The introduction of the 2,3,6,7-tetrahydro-1*H*,5*H*,11*H*-pyrano[2,3-*f*]pyrido[3,2,1-*ij*]quinolin-11-

For internal use, please do not delete. Submitted_Manuscript

one fluorophore (cf. Scheme 1, fluorescent probe **8**) should result in a slightly red-shifted λ_{max} compared with the 7-diethylaminocoumarin derivatives.^[7c] A higher red-shifted λ_{max} should be observed with **9**, where a π -extended coumarin (8-(dimethylamino)-2*H*-benzo[*g*]chromen-2-one) moiety is the fluorophore (cf. Scheme 1).^[9] Overall, we synthesized fluorescent probes **1**, **3**, **4**, **5**, **8** and **9** with the same 1,4-triazole linkage between the ionophore and the fluorophore, as shown in fluorescent probe **2** (cf. Scheme 1), to take advantage of the higher Na^+/K^+ selectivity and the higher Na^+ -induced fluorescence enhancement (FE). Further, for comparison, we synthesized the free aza-15-crown-5 fluorescent dye the 7-(diethylamino)-3-(4-phenyl-1*H*-1,2,3-triazol-1-yl)-2*H*-chromen-2-one (**7**) according to the literature^[10] (see Scheme 1).

Syntheses of 1,2,3-triazol-1,4-diyl – fluoroionophores: To build up **1**, **3**, **4**, **5**, **8** and **9**, we synthesized according to the literature the alkynes **10**^[11a], **13**^[11b] and **14**^[8] (cf. Scheme 1). Further, alkynes **11** and **12** were synthesized from the corresponding aldehydes^[3b,5a] by using dimethyl-1-diazo-2-oxopropylphosphonate.^[12] Coupling of alkyne compounds **10-14** with the respective coumarin-azides^[10,13] by using the well-established CuAAC-reaction^[14a,b], afforded fluoroionophores **1**, **3**, **4**, **5**, **8** and **9** (Scheme 1).

Spectroscopic properties of 1-9 in CH_3CN : The UV/Vis absorption spectra of fluoroionophores **1**, **3**, **4**, **8** and **9** exhibit two charge transfer (CT) bands in CH_3CN (see Figures S1-S4, S6 and S7), as already found for fluoroionophore **2**.^[8] The long-wavelength CT absorption for the diethylaminocoumarin derivatives **1-5** centered at around 410 nm and for **8** and **9** at around 430 nm in CH_3CN . The second CT absorption band, which is typical for π -conjugated anilino-1,2,3-triazol-1,4-diyl – fluoroionophores, can be found for **1-4**, **8** and **9** at around 290 nm in CH_3CN corresponding to a CT from the nitrogen lone pair of the aromatic ring (donor) to the 1,2,3-triazole acceptor unit. Based on this band, it is possible to evaluate the conjugation of the nitrogen lone pair with the aromatic ring. In the series of **1-4**, **8** and **9**, we found for **1** the most intense CT absorption at around 290 nm (Figure 1a) with an extinction coefficient of $31000 \text{ M}^{-1}\cdot\text{cm}^{-1}$. The fluoroionophores **2**, **3**, **4**, **8** and **9** displays a CT absorption at ~ 290 nm with a lower extinction coefficient (cf. Figure 1a and 1b). The different aza-15-crown-5 units in **2**, **3**, **4**, **8** and **9** are not so flexible as in **1**, caused by the steric hindrance of the substituent in ortho position as in **2**, **3**, **8** and **9** or by the directly in ortho position linked aza-15-crown-5 unit, as shown in **4**. As a consequence, in **2**, **3**, **4**, **8** and **9** the C-N bond between the aza-15-crown-5 unit and the aromatic ring is twisted and this excludes a complete conjugation of the nitrogen lone pair with the aromatic ring. Therefore, **1** possesses a better electron donor unit as **2**, **3**, **4**, **8** and **9** caused by the more efficient conjugation of the nitrogen lone pair with the aromatic ring. Further, the reference compounds **5** and **7**, without an anilino unit, showed the typical coumarin CT absorption band at around 410 nm in CH_3CN , but no CT absorption at around 290 nm (cf. Figures S5a and S5b).

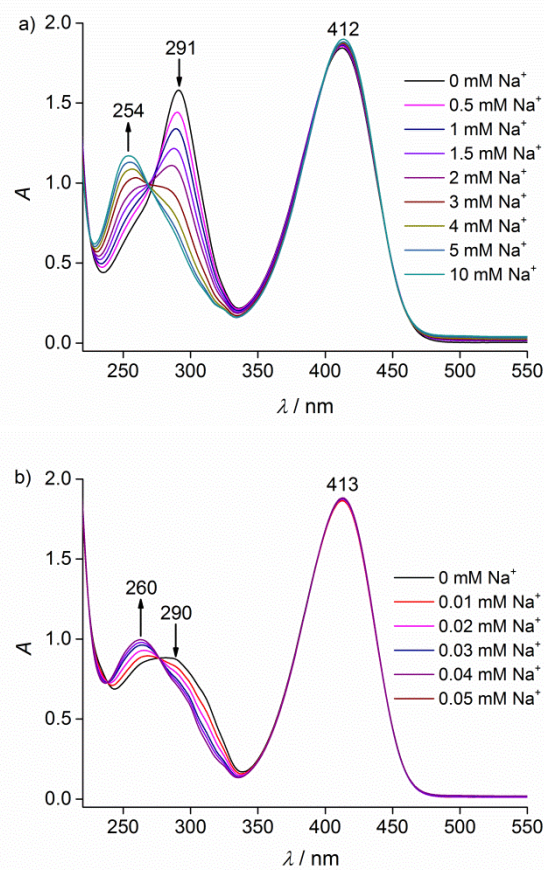


Figure 1. UV/Vis absorption spectra of a) **1** ($c = 5 \cdot 10^{-5} \text{ M}$) and b) **2** ($c = 5 \cdot 10^{-5} \text{ M}$) in the presence of different Na^+ concentrations in CH_3CN .

Spectroscopic properties of 1-5, 8 and 9 + Na^+ and K^+ in CH_3CN : In the next step, we studied the influence of Na^+ and K^+ towards the UV/Vis absorption of **1-5**, **8** and **9** in CH_3CN . For **1-5**, **8** and **9**, we found no change of the long-wavelength absorption in the presence of Na^+ or K^+ (cf. Figures S1a-S7a). In general for **1-4**, **8** and **9** the complexation of Na^+ and K^+ can be seen from the CT absorption at around 290 nm (see Figures S1a-S4a, S6a and S7a). We observed for **1-4**, **8** and **9** a decrease of the CT band at 290 nm in the presence of Na^+ and an increase of the absorption at ~ 260 nm. However, for **1-4**, **8** and **9** + K^+ , we observed only a small change of the CT band (cf. Figure S1b-S4b, S6b and S7b). The resulting UV/Vis absorption spectra of **1-4** + Na^+ were similar to the anilino free reference compounds **5** and **7**, respectively (cf. Figure S5a and S5b). Thus, Na^+ decreases the donor ability of the anilino unit in **1-4**, **8** and **9** which leads to a decrease of the CT absorption band. We found for **1-4** + Na^+ a different pronounced reduction of the CT band, depending on the nature of the aza-15-crown-5 unit and on the conjugation of the nitrogen lone pair with the aromatic ring. For **1**, we observed the strongest decrease of the CT band (see Figure 1a) and a smaller Na^+ -induced CT reduction at 290 nm for **2**, **3** and **4**, respectively (cf. Figures 1b, S3a and S4a). However, for

For internal use, please do not delete. Submitted_Manuscript

2, 4, 8 and **9**, we found at ~ 0.05 mM Na^+ a complete decrease of the short wavelength CT absorption and for **1** and **3** at a higher Na^+ concentration of ~ 5 mM. Thus, **2, 4, 8** and **9** formed more stable Na^+ -complexes than **1** and **3** in CH_3CN . Consequently, the aza-15-crown-5 moiety and the alkoxy substituent in ortho position were responsible for enhanced Na^+ -complex stabilities.

Table 1. Photophysical properties of **1-9** in CH_3CN .^[a]

	λ_{abs} [nm]	λ_{f} [nm]	$\phi_{\text{f}}^{\text{[b]}}$	$FEF^{\text{[c]}}$	$K_{\text{d}}^{\text{Na}^+ \text{[d]}}$ [μM]
1	412	485	0.014	-	-
1 + Na⁺	412	485	0.685	46.5	867
1 + K⁺	412	485	0.052	3.7	1378
2	413	484	0.130	-	-
2 + Na⁺	413	484	0.307	2.2	5
2 + K⁺	413	484	0.235	1.4	16
3	411	486	0.082	-	-
3 + Na⁺	411	486	0.440	5.4	770
3 + K⁺	411	486	0.146	1.8	4454
4	413	484	0.152	-	-
4 + Na⁺	413	484	0.667	4.3	12
4 + K⁺	413	484	0.279	1.8	33
5	412	483	0.762	-	-
5 + Na⁺	412	483	0.765	1.0	-
5 + K⁺	412	483	0.767	1.0	-
6	410	493	0.017	-	-
7	413	483	0.702	-	-
8	430	500	0.475	-	-
8 + Na⁺	430	500	0.712	1.5	6
8 + K⁺	430	500	0.532	1.1	33
9	431	591	0.221	-	-
9 + Na⁺	431	591	0.375	1.6	7
9 + K⁺	431	591	0.265	1.2	15

[a] All data were measured in CH_3CN in the absence and presence of NaPF_6 or KPF_6 , respectively. [b] Fluorescence quantum yield, (± 15)%. [c] Fluorescence enhancement factor, [$FEF = I/I_0$], (± 0.2). [d] Dissociation constants K_{d} for Na^+ -complexes.

The fluorescence spectra of **1-7** showed emissions centered at around 485 nm in CH_3CN (cf. Table 1). Thus, the fluorophore moiety adjusted λ_{max} , but we found for probes **1-7** different quantum yields ϕ_{f} (cf. Table 1). Overall, the ϕ_{f} of **1-4** were lower

than that of the aza-15-crown-5-free fluorescent probe **7** ($\phi_{\text{f}} = 0.702$). The low ϕ_{f} of probes **1-4** (cf. Table 1) suggests that a photoinduced electron transfer (PET) takes place in **1-4**, which quenches the fluorescence, as already observed for the highly K^+/Na^+ selective 1,2,3-triazol-fluoroionophores^[7a-d]. There, we investigated the influence of the isomeric triazole linkage towards the ϕ_{f} .^[7a,b] Herein, the PET process is influenced by the ionophore moiety. In the series of **1-4**, which are substituted with the diethylaminocoumarin fluorophore, we observed following trend of the ϕ_{f} : 0.152 (**4**) > 0.130 (**2**) > 0.082 (**3**) > 0.014 (**1**), cf. Table 1. As discussed vide supra, in **2, 3** and **4** the nitrogen lone pair is not fully conjugated with the aromatic ring caused by the steric hindrance of the substituent in ortho position as found for **2** and **3** or by the directly in ortho position linked aza-15-crown-5 unit, as shown in **4**. In a more flexible arrangement, such as in **1**, the nitrogen lone pair of the anilino unit is mostly conjugated with the phenyl ring and this acts as an efficient PET donor. Thus, the anilino unit in **1** is a better PET donor than in **2, 3** and **4**. In addition to it, the low ϕ_{f} value of **1** (0.014) is comparable with the ϕ_{f} value of the flexible diethylaminophenyl substituted 1,2,3-triazol-coumarin derivative **6**^[7a] (0.017, see Scheme 1). In contrast to **1**, the benzo-15-crown-5 substituted fluoroionophore **5** exhibits a ϕ_{f} value of 0.762, which is comparable with the ϕ_{f} value of the reference compound **7** ($\phi_{\text{f}} = 0.702$).

To substantiate the influence of the ionophore moieties towards the fluorescence quenching in **1, 2** and **4**, we measured the redox properties of **1, 2, 4, 5** and **7** in CH_3CN . The Rehm-Weller equation allows the estimation of the thermodynamic driving force for the PET process ΔG_{PET} .^[15,16] The fluoroionophores **1, 2, 4, 5** and **7** have nearly the same reduction potential E_{Red} (-1.90 V) and the same energy difference between the ground and the excited state E_{00} (2.77 eV), but they differ in the oxidation potential E_{Ox} , caused by the different electron donor capabilities of the ionophore moieties. We found for **1** a E_{Ox} of 0.75 V, for **2** a 0.77 V and for **4** a 0.80 V, respectively. Hence, we estimated for **1, 2** and **4** the following ΔG_{PET} values: -0.22 eV, -0.20 eV and -0.17 eV, respectively. Herein, within **1, 2** and **4** a reductive PET from the anilino donor to the diethylaminocoumarin acceptor takes place, as indicated by negative ΔG_{PET} values.^[16] The more negative the ΔG_{PET} value, the more likely the fluorescence quenching, as found in **1, 2** and **4** (cf. Table 1). In opposite, we found for **5** and **7** a E_{Ox} of 1.30 V and 1.36 V, respectively. Therefore, we calculated positive ΔG_{PET} values of +0.33 eV and +0.39 eV. Thus, in **5** ($\phi_{\text{f}} = 0.762$) and **7** ($\phi_{\text{f}} = 0.702$) no reductive PET can take place, which quenches the fluorescence. Hence, in this series **1-5**, the fluorescence is effectively quenched within **1**.

Further, we observed in CH_3CN a red-shift of λ_{max} for **8** and **9** compared with the diethylaminocoumarin derivatives **1-4**. The λ_{max} of **8** was found at 500 nm and of **9** at 591 nm, respectively. Herein, the *N*-(*o*-methoxyphenyl)aza-15-crown-5 substituted fluoroionophores **8** ($\phi_{\text{f}} = 0.475$) and **9** ($\phi_{\text{f}} = 0.221$) showed, as also found for **2**, high ϕ_{f} values. This result confirms the influence of the bulky methoxy group in ortho position towards the fluorescence quenching process in **2, 8** and **9**, as discussed vide supra.

For internal use, please do not delete. Submitted_Manuscript

To validate the Na⁺ sensing capabilities of **1-5**, **8** and **9** we investigated the influence of Na⁺ and K⁺ on the fluorescence intensity of **1-5**, **8** and **9** in CH₃CN. Initially, we performed titration experiments with **1-5**, **8** and **9** only in the presence of Na⁺. Overall, for **1-4**, **8** and **9** we observed a FE in the presence of Na⁺ (representative for **1-4**, **8** and **9** see Figure 2), but we found for **5** + Na⁺ no change of the fluorescence intensity. In summary, Figure 3a shows the titration curves of **1**, **3** and **5** + Na⁺ and Figure 3b of **2**, **4**, **8** and **9** + Na⁺ at λ_{\max} nm in CH₃CN. Herein, **1** showed the highest Na⁺-induced FE by a factor of 46.5. The maximal FE of the *N*-phenylaza-15-crown-5 substituted fluoroionophores **1** was reached in the presence of 5 mM Na⁺ (cf. Figure 3a). For **1** + Na⁺, we determined a high ϕ_f value of 0.685 (cf. Table 1). As mentioned above, the fluoroionophores **2**, **3**, **4**, **8** and **9** exhibited higher ϕ_f values as **1**. Overall, the ϕ_f values of **2**, **3**, **4**, **8** and **9** + Na⁺ were higher than of the Na⁺-free solutions (cf. Table 1). However, we observed smaller Na⁺-induced FE factors for **2** (FEF = 2.2), **3** (FEF = 5.4), **4** (FEF = 4.3), **8** (FEF = 1.5) and **9** (FEF = 1.6). The maximal FE was reached for **2**, **4**, **8** and **9** at a Na⁺ concentration of 0.05 mM (see Figure 3b), but for **3** only at 5 mM Na⁺ (Figure 3a). The Na⁺ induced FEFs of **1-4**, **8** and **9** can be explained by an off switching of the PET quenching process by Na⁺. We assume, that Na⁺ enhances the oxidation potential of the ionophore moiety, as already observed for several π -conjugated anilino-1,2,3-triazol-1,4-diyl – fluoroionophores for K⁺^[7a-d] and a set of aza-15-crown-5 substituted Na⁺ fluoroionophores.^[3c,4a,b,5c] Therefore, the ΔG_{PET} value becomes more positive and the PET is more unlikely. This results in an on switching of the fluorescence.

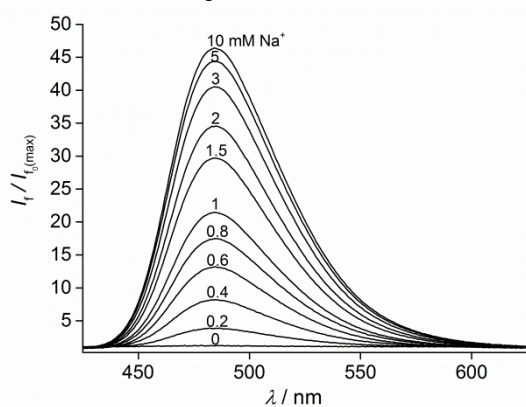


Figure 2. Fluorescence spectra of **1** ($c = 5 \cdot 10^{-6}$ M, $\lambda_{\text{ex}} = 410$ nm) in the presence of different Na⁺ concentrations in CH₃CN.

To compare the Na⁺-complex stabilities of **1-4**, **8** and **9** in CH₃CN, we determined the K_d values based on the Na⁺-induced FEFs.^[13] The resulting K_d values of **1-4**, **8** and **9** + Na⁺ can be divided into two groups. On the one hand, **1** and **3** + Na⁺ possess K_d values of 867 μ M and 770 μ M and on the other hand **2**, **3**, **8** and **9** + Na⁺ showed K_d values of 5 μ M, 12 μ M, 6 μ M and 7 μ M, respectively (cf. Table 1). Thus, we found for **2**, **8** and **9** + Na⁺ the most stable Na⁺-complexes. In these Na⁺-complexes, the aza-15-crown-5 is orientated orthogonal to the phenyl ring into the direction of the methoxy group.^[4a,b] Here, Na⁺ is bound via

six donor atoms including five O-atoms and one N-atom. Thus, the bulky methoxy group in **2**, **8** and **9** prevents as mentioned above a complete fluorescence quenching, but enhances the Na⁺-complex stability. Noticeable, the diaza-15-crown-5 moiety in **3** binds Na⁺, as well as the monoaza-15-crown-5 moiety in **1**, suggesting that the methoxy groups in ortho position were not involved in the coordination sphere with Na⁺ in CH₃CN. Overall, the Na⁺-complex stability is influenced by the ionophore moiety in CH₃CN.

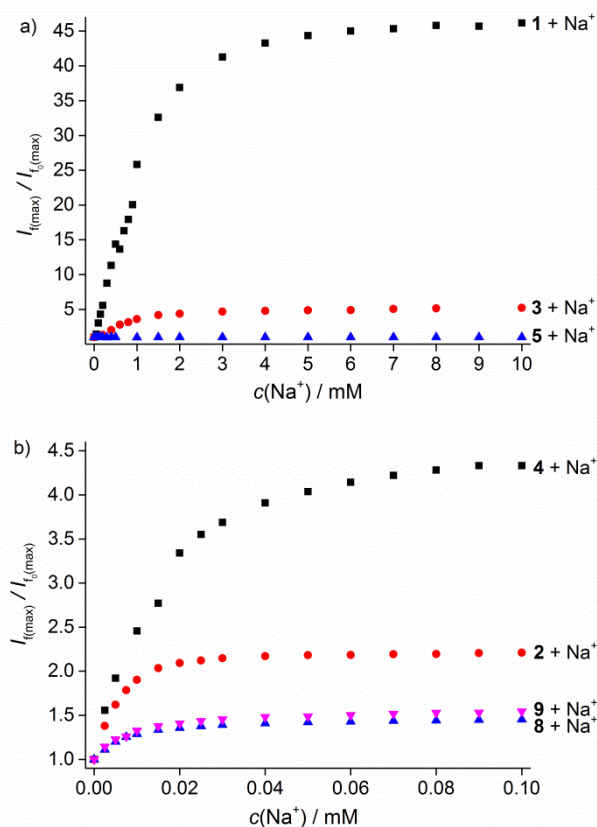


Figure 3. Fluorescence enhancement factors in the presence of Na⁺ for a) **1**, **3** and **5** and b) for **2**, **4**, **8** and **9** at λ_{\max} .

In the next step, we investigated the influence of competing K⁺ ions on the fluorescence intensity of **1-4** in CH₃CN. In all cases, K⁺ enhances the fluorescence intensity of **1-4**, but much weaker than for Na⁺ (cf. Table 1 and Figure 4). As expected, **5** + K⁺ showed no change of the fluorescence.

Overall, as required for an effective Na⁺ sensing, **1** showed a moderate Na⁺/K⁺ selectivity, a high Na⁺ induced FE, a high ϕ_f of the Na⁺-complex and a K_d value of 867 μ M in CH₃CN.

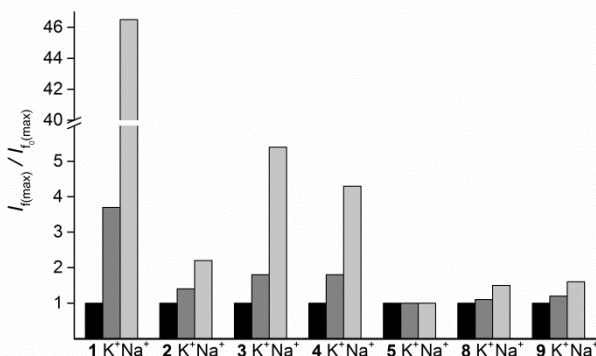


Figure 4. Fluorescence enhancement factors of 1-5, 8 and 9 (black bars) at λ_{\max} in the presence of maximal K^+ (grey bars) and Na^+ (light grey bars) concentration (cf. Figure 3) in CH_3CN .

Spectroscopic properties of 4, 8 and 9 + Na^+ and K^+ in $H_2O/DMSO$ (v/v 99/1) mixture: To ensure the solubility of 1, 3, 4, 8 and 9 in an aqueous milieu, we prepared solutions with different fluoroionophore concentrations in the range of 5×10^{-5} M to 10^{-6} M in a $H_2O/DMSO$ mixture of 99/1 (v/v). Herein, we only found for 4, 8 and 9 a complete solubility in a $H_2O/DMSO$ mixture of 99/1 (v/v) up to a fluoroionophore concentration of $\sim 1.5 \times 10^{-5}$ M (cf. Figures S22a-c). However, the fluorescent probes 1 and 3 showed in a concentration range from 5×10^{-5} M to 10^{-6} M no adequate solubility in various $H_2O/DMSO$ mixtures (99/1, 9/1, 3/1 or 1/1 (v/v)).^[13] Thus, the titration experiments with NaCl and KCl were carried out only with 4, 8 and 9 ($c = 10^{-5}$ M) under simulated physiological conditions (10 mM Tris-buffer, pH 7.2, $H_2O/DMSO$ (v/v 99/1)). The fluorescence emission of the diethylaminocoumarin substituted fluoroionophore 4 centered, as also found for 2, at 500 nm. A slightly red-shifted λ_{\max} was observed for 8 at 517 nm and a higher red-shifted λ_{\max} showed 9 at 613 nm. However, the ϕ_f of 2 ($\phi_f = 0.009$) and 4 ($\phi_f = 0.014$) were similar to each other. Herein, the fluorescence quenching within the diethylaminocoumarin substituted fluoroionophores 2 and 4 is not only influenced by the ionophore moiety and therefore by the PET process, as mentioned above in CH_3CN , but rather by H_2O . H_2O itself quenches the fluorescence of the diethylaminocoumarin fluorophore, as already found for diethylaminocoumarin derivatives^[17] and for the reference compound 7 ($\phi_f = 0.106$, cf. Table 1 and 2). Likewise, H_2O reduces also the ϕ_f of 7-(diethylamino)-3-(4-phenyl-1*H*-1,2,3-triazol-1-yl)-2*H*-chromen-2-one derivatives.^[9] Thus, we found for 9 a very low ϕ_f of 0.002. Furthermore, a higher ϕ_f value of 0.025 showed 8 containing of a 2,3,6,7-tetrahydro-1*H*,5*H*,11*H*-pyrano[2,3-*f*]pyrido[3,2,1-*ij*]quinolin-11-one fluorophore. These coumarin derivatives exhibited even in H_2O high ϕ_f values up to 0.95.^[18] Concluding that in 8, the fluorescence is effectively quenched by a PET process, as required for an effective Na^+ sensing.

In the next step, we carried out titration experiments with 4, 8 and 9 in the presence of NaCl under simulated physiological conditions. Figure 5 depicts the fluorescence of 8, representative

for 4, 8 and 9, in the presence of increasing Na^+ concentrations. Figure 6 diagrammed the titration curves of 4, 8 and 9 with Na^+ at λ_{\max} , respectively. In all cases, we observed a Na^+ -induced FE, but the maximal FE was reached at different Na^+ concentrations. Thus, for 4 at 500 mM NaCl with a FEF of 6.6, for 8 at 500 mM NaCl with a FEF of 10.9 and for 9 at 1000 mM NaCl with a FEF of 2.0. Further, we carried out titration experiments with 4, 8 and 9 in the presence of KCl. As expected, K^+ showed a smaller influence on the fluorescence of 4, 8 and 9. We observed for 4 + 500 mM K^+ a FEF of 3.4, for 8 + 500 mM K^+ a FEF of 2.7 and for 9 + 1000 mM K^+ a FEF of 1.1. We found for 9 the highest Na^+/K^+ selectivity and for 4 a poor Na^+/K^+ selectivity.

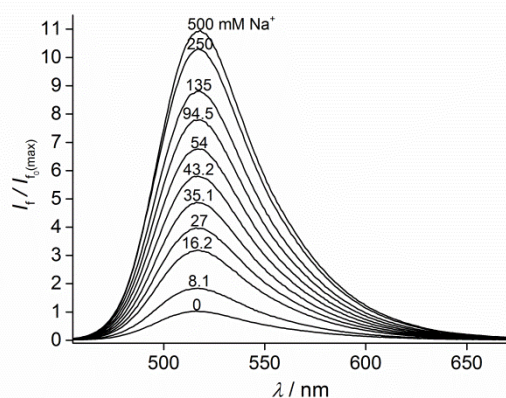


Figure 5. Fluorescence spectra of 8 ($c = 10^{-5}$ M, $\lambda_{\text{ex}} = 440$ nm) in the presence of different Na^+ concentrations in a $H_2O/DMSO$ (99/1 v/v) mixture with 10 mM Tris buffer (pH = 7.2).

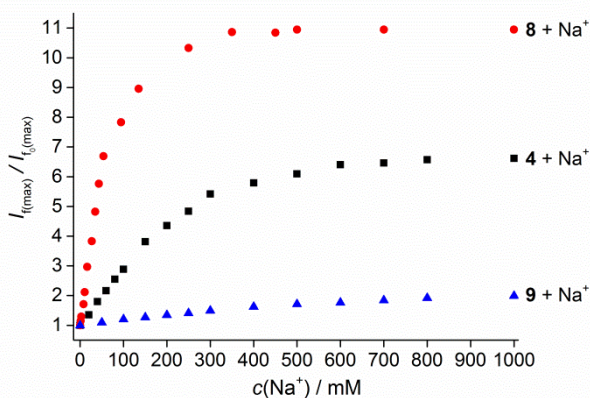


Figure 6. Fluorescence enhancement factors of 4, 8, and 9 in the presence of Na^+ concentrations in a $H_2O/DMSO$ (99/1 v/v) mixture with 10 mM Tris buffer (pH = 7.2).

Again, the high Na^+/K^+ selectivity of 9 can be also seen from the UV/Vis absorption spectra of 9 + Na^+ and K^+ in H_2O . Here, only Na^+ reduces the CT band of 9 at around 300 nm (Figure S8c). In contrast to 9 + K^+ , 4 and 8 showed also a K^+ -reduced CT absorption at around 300 nm (cf. Figures S8a and S8b).

For internal use, please do not delete. Submitted_Manuscript

Dissociation constants (K_d) of fluorescent probes **4** + Na⁺, **8** + Na⁺ and **9** + Na⁺ were calculated from plots of fluorescence intensities of **2**, **8** and **9** versus Na⁺ ion concentrations.^[13] In all cases, we observed a 1:1 complexation between **4**, **8** and **9** with Na⁺, indicated by the slopes (-1) of the plots.^[13] For **4** + Na⁺, **8** + Na⁺ and **9** + Na⁺, we found K_d values of 155 mM, 48 mM and 223 mM, respectively (cf. Table 2). Herein, **4** and **2** consisting of different Na⁺ ionophores, but they showed the nearest K_d values (**2** + Na⁺, K_d = 117 mM, **4** + Na⁺, K_d = 155 mM). For a set of fluoroionophores, which were all equipped with the *N*-methylacetate-aza-15-benzo-crown-5 ionophore (cf. **4**), but with different fluorophore moieties, were found a wide range of K_d values for Na⁺, which differed from 89 mM to 226 mM.^[5a] Furthermore, the *N*-(*o*-methoxyphenyl)aza-15-crown-5 based fluoroionophores **2**, **7** and **9** showed also different K_d values for Na⁺ in the following order **9** > **2** > **8**.

Interestingly, we found that with an increased Na⁺-complex stability in the following order: **8** (48 mM) > **2** (117 mM) > **9** (223 mM), the Na⁺ induced FE of **8** (FEF = 10.9) > **2** (FEF = 5.0) > **9** (FEF = 2.0) is also increased. Further, **8** formed the strongest Na⁺-complex, but also complexes to K⁺ (FEF = 2.7). A negligible K⁺ influence showed fluorescent probe **9** but also a smaller Na⁺ induced FE. Thus, the Na⁺/K⁺ selectivity is decreased in the order **9** < **2** < **8**.

Again, we tested the suitability of **8** to measure Na⁺ in the presence of physiological relevant K⁺ levels. Thus, we prepared different Na⁺ solutions, containing 10 mM KCl or 135 mM KCl to simulate the extra- or intracellular K⁺ background, respectively. As found for **8** + Na⁺ the K_d value in K⁺-free solutions is 48 mM. Herein, the K_d value of **8** + Na⁺ in the presence of 10 mM K⁺ (K_d = 45 mM) or 135 mM K⁺ (K_d = 42 mM) is slightly influenced by K⁺ (see Figure S18a and S19a). However, we observed different Na⁺-induced FEs, depending on the adjusted K⁺ concentration. For **8** + Na⁺ in the presence of 10 mM K⁺, we found a FEF of 10.2 and in the presence of 135 mM a FEF of 5.5 (Figure S18b and S19b). Thus the performance of **8** is only slightly influenced by extracellular K⁺ levels.

The Na⁺-selectivity of fluorescent probes **8** and **9** was verified by titration experiments with other metal ions. Particularly, we focused on biological cations such as K⁺, Ca²⁺, Mg²⁺, Li⁺, Ni²⁺, Cu²⁺ and Zn²⁺ at their physiological concentrations (Figure 7a for **8** and 6b for **9**). These cations show only negligible effects on the fluorescence of **8** and **9**. Moreover, **8** and **9** recognized Na⁺ even in the co-presence of these metal ions, as shown in Figure 7a and 7b. Therefore, **8** and **9** were capable fluorescent probes to determine extracellular Na⁺ levels in the presence of other biological important cation concentrations.

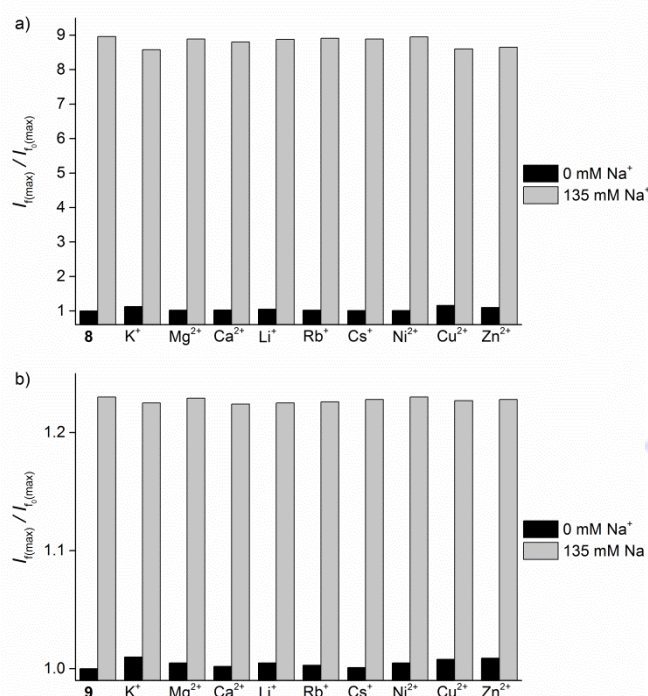


Figure 7. Fluorescence intensities changes of a) **8** ($c = 10^{-5}$ M, $\lambda_{\text{ex}} = 440$ nm, 10 mM Tris buffer, pH = 7.2) at 517 nm and b) **9** ($c = 10^{-5}$ M, $\lambda_{\text{ex}} = 420$ nm, 10 mM Tris buffer, pH = 7.2) at 613 nm in the presence of 10 mM for K⁺, 2 mM for Mg²⁺, Ca²⁺, Li⁺, Rb⁺, Cs⁺ and 100 μ M for Ni²⁺, Cu²⁺, Zn²⁺ (black bars) and subsequent addition of 135 mM of Na⁺ (grey bars).

To verify the pH sensitivity of **8** and **9**, we measured the fluorescence at different pH values.^[13] Thus, we found only minor effects towards the sensitivity of **8** or **9** at various concentrations of Na⁺ ions within the pH range from 6.8 to 8.8 (see Figures S21a and S21b).

Table 1. Photophysical properties of **2**, **4**, **7**, **8** and **9** in H₂O.^[a]

	λ_{abs} [nm]	λ_{f} [nm]	$\phi^{\text{[b]}}$	FEF ^[c]	$K_d^{\text{[d]}}$ [mM]
2 ^[e]	422	500	0.009	-	-
2 + Na ⁺	422	500	0.048	5.0	117
2 + K ⁺	422	500	0.017	1.5	276
4	423	500	0.014	-	-
4 + Na ⁺	423	500	0.093	6.6	155
4 + K ⁺	423	500	0.048	3.4	270
7	424	501	0.106	-	-
8	440	517	0.025	-	-
8 + Na ⁺	440	517	0.275	10.9	48
8 + K ⁺	440	517	0.067	2.7	68

9	418	613	0.002	-	-
9 + Na ⁺	418	613	0.004	2.0	223
9 + K ⁺	418	613	0.002	1.1	[^f]

[a] All data were measured in H₂O/DMSO mixtures (v/v, 99/1) in 10 mM Tris buffer (pH = 7.2) and in the absence and presence of 1 M NaCl or 1 M KCl. [b] Fluorescence quantum yield, (\pm 15)%. [c] Fluorescence enhancement factor, [$FEF = I/I_0$], (\pm 0.2). [d] Dissociation constants K_d for Na⁺- or K⁺- complexes. [e] See reference [8] for **2**. [f] The fluorescence intensity changes were too weak to determine the K_d value of **9** + K⁺ accurately.

Conclusions

In summary, we have synthesized a set of Na⁺-responsive fluoroionophores **1**, **3**, **4**, **5**, **8** and **9**. At first, we found that the flexibility of the aza-15-crown-5 moiety influences obviously the fluorescence quenching process within **1-4**, **8** and **9** in CH₃CN. Particularly, the conjugation of the nitrogen lone pair with the aromatic ring determines the donor ability of the ionophore moiety and therefore the PET efficiency within **1-4**, **8** and **9**. Herein, **1** exhibited a low ϕ_f of 0.014 in CH₃CN, as required for an effective Na⁺ sensing. Thus, **1** showed the highest Na⁺-induced FEF of 44.5 and **1** + Na⁺ exhibited a K_d value of 867 μ M in CH₃CN. However, the most stable Na⁺-complexes formed the *N*-(*o*-methoxyphenyl)aza-15-crown-5 based fluoroionophores **2**, **8** and **9** with K_d values of 5 μ M, 6 μ M and 7 μ M in CH₃CN. Herein in CH₃CN, the Na⁺-complex stability is influenced by the ionophore moiety. Secondly, the *N*-(*o*-methoxyphenyl)aza-15-crown-5 based fluoroionophores **2**, **8** and **9** showed different K_d values and Na⁺/K⁺ selectivities in H₂O. The most stable Na⁺-complex formed **8** + Na⁺ with a K_d value of 48 mM, but showed a small K⁺ induced FE at intracellular K⁺ concentrations. A higher Na⁺/K⁺ selectivity exhibited fluorescent probe **9**, but also a higher K_d value of 223 mM. Thus, fluorescent probe **8** is a suitable tool to monitor selective physiological Na⁺ levels in the presence of extracellular K⁺ concentrations. Further, **9** is a highly Na⁺/K⁺ selective fluoroionophore capable to visualize extracellular Na⁺ concentrations. Overall, we have shown that not only the *N*-(*o*-methoxyphenyl)aza-15-crown-5 ionophore specified the Na⁺-complex stability and Na⁺/K⁺ selectivity, but also the fluorophore moiety influences the Na⁺ binding properties.

Experimental Section

General Methods and reagents: All commercially available chemicals were used without further purification. Solvents were distilled prior use. ¹H and ¹³C NMR spectra were recorded on 300 MHz or 500 MHz instruments, respectively. Data are reported as follows: chemical shifts in ppm (δ), multiplicity (s = singlet, d = doublet, t = triplet, dd = doublet of doublets, m = multiplet), integration, coupling constant (Hz). ESI spectra were recorded using a Micromass Q-TOF micro mass spectrometer in a positive electrospray mode. Column chromatography was performed with silica gel (Merck; silica gel 60 (0.04-0.063 mesh)).

General synthetic procedures for **11 and **12**:** To a mixture of the corresponding aldehyde derivatives (*N,N*-bis(*o*-methoxyphenyl)diaza-15-crown-5-aldehyde^[3b] or *N*-methylacetate-aza-15-benzo-crown-5-aldehyde^[5a]) (2.43 mmol) and 673 mg (4.86 mmol) K₂CO₃ in 35 mL dry methanol was added 564 mg (2.93 mmol) dimethyl-1-diazo-2-oxopropylphosphonate^[12]. This suspension was stirred for 20 hours at room temperature. After addition of 60 mL CHCl₃, the organic layer was extracted with water (10 mL), separated, dried with MgSO₄ and concentrated in vacuo. The resulting residue was purified by column chromatography on silica with CHCl₃/CH₃OH (v/v, 95/5) as an eluent mixture to afford **11** or **12** as pale oils.

***N*-(4-Ethynyl-2-methoxyphenyl)-*N'*-(2-methoxyphenyl)diaza[15]crown-5 ether (**11**):** Yield 37% (408 mg); ¹H NMR (CDCl₃, 300 MHz): δ = 7.05-6.81 (m, 7H), 3.81 (s, 3H), 3.79 (s, 3H), 3.63-3.38 (m, 20H), 3.02 ppm (s, 1H); ¹³C NMR (CDCl₃, 75 MHz): δ = 153.19, 151.78, 140.35, 139.05, 125.21, 122.55, 121.51, 120.64, 119.87, 115.28, 114.46, 111.82, 84.14, 75.71, 70.40, 70.34, 69.54, 69.50, 69.45, 69.35, 55.44, 55.33, 52.73, 52.60, 52.45, 52.33 ppm; HRMS (ESI): m/z calcd for C₂₆H₃₄N₂O₅+H⁺: 455.2546 [M +H⁺]; found: 455.1314.

***N*-Methylacetate-aza-4-ethynylbenzo[15]crown-5 ether (**12**):** Yield 45% (396 mg); ¹H NMR (CDCl₃, 300 MHz): δ = 7.02 (dd, J = 8.2, 1.4 Hz, 1H), 6.92 (d, J = 1.4 Hz, 1H), 6.79 (d, J = 8.2 Hz, 1H), 4.15 (s, 2H), 4.13-4.10 (m, 2H), 3.88-3.86 (m, 2H), 3.78 (t, J = 5.9 Hz, 2H), 3.72-3.60 (m, 11H), 3.50 (t, J = 5.9 Hz, 2H), 2.99 ppm (s, 1H); ¹³C NMR (CDCl₃, 75 MHz): δ = 171.99, 150.61, 140.84, 125.59, 119.40, 116.62, 114.89, 84.05, 75.71, 70.89, 70.62, 70.26, 70.09, 69.54, 69.09, 68.50, 53.21, 52.10, 51.55 ppm; HRMS (EI): m/z calcd for C₁₉H₂₅N₂O₆: 363.1682 [M]; found: 363.1644.

General CuACC procedure for **1, **3**, **4**, **5**, **8** and **9**:** A mixture of the corresponding alkynyl substituted crown compound **10**^[11a], **11**, **12**, **13**^[11b] or **14**^[6] (0.415 mmol) and the corresponding azidocoumarin derivatives^[10] (0.415 mmol) or the π -extended azidocoumarin derivative^[13] (0.415 mmol), CuSO₄·5H₂O (5.3 mg) and sodium ascorbate (8.2 mg) in 9 mL THF/H₂O (v/v, 2/1) was stirred at 60 °C for 48 hours. After that 5 mL H₂O were added to the mixture and then extracted with CHCl₃ (30 mL). The organic layer was dried with MgSO₄ and concentrated in vacuo. The residue was purified by column chromatography on silica using CHCl₃/CH₃OH (v/v, 99/5) as an eluent mixture to afford **1**, **3-5** as yellow solids, **8** as an orange solid and **9** as a red solid.

3-(4-(4-(1,4,7,10-tetraoxa-13-azacyclopentadecan-13-yl)phenyl)-1*H*-1,2,3-triazol-1-yl)-7-(diethylamino)-2*H*-chromen-2-one (1**):** Yield 20% (48 mg); M.p.: 168°C (decomp.); ¹H-NMR (CDCl₃, 300 MHz): δ = 8.65 (s, 1H), 8.42 (s, 1H), 7.75 (d, J = 8.3 Hz, 2H), 7.41 (d, J = 8.9 Hz, 1H), 6.77-6.64 (m, 3H), 6.56 (d, J = 2.0 Hz, 1H), 3.78 (d, J = 5.5 Hz, 4H), 3.66 (q, J = 9.4 Hz, 16H), 3.45 (q, J = 7.0 Hz, 4H), 1.24 ppm (t, J = 7.0 Hz, 6H); ¹³C-NMR (CDCl₃, 75 MHz): δ = 156.96, 155.68, 151.39, 148.02, 147.55, 134.16, 129.89, 127.01, 118.71, 118.05, 117.20, 111.59, 109.98, 107.21, 97.02, 71.30, 70.22, 70.17, 68.56, 52.54, 44.95, 12.42 ppm; HRMS (ESI): m/z calcd for C₃₁H₃₉N₅O₆+H⁺: 578.2979 [M +H⁺]; found: 578.2933.

7-(diethylamino)-3-(4-(3-methoxy-4-(13-(2-methoxyphenyl)-1,4,10-trioxo-7,13-diazacyclopentadecan-7-yl)phenyl)-1*H*-1,2,3-triazol-1-yl)-2*H*-chromen-2-one (3**):** Yield 75% (221 mg); M.p.: 45°C (decomp.); ¹H NMR (CDCl₃, 500 MHz): δ = 8.70 (s, 1H), 8.38 (d, J = 3.1 Hz, 1H), 7.45-7.30 (m, 3H), 7.08-6.80 (m, 5H), 6.64-6.61 (m, 1H), 6.53-6.50 (m, 1H), 3.90-3.38 (m, 30H), 1.20 ppm (t, J = 6.9 Hz, 6H); ¹³C NMR (CDCl₃, 125 MHz): δ = 156.78, 155.59, 153.07, 152.94, 151.33, 147.50, 134.26, 134.21, 129.85, 121.35, 120.90, 120.58, 119.57, 118.19, 116.83, 111.70, 109.89, 109.86, 109.17, 106.96, 96.81, 75.03, 74.83, 70.43, 70.34, 70.28, 69.42, 55.51, 55.27, 52.64, 52.59, 52.50, 52.44, 44.83, 17.13, 12.29

For internal use, please do not delete. Submitted_Manuscript

ppm; HRMS (ESI): m/z calcd for $C_{39}H_{48}N_6O_7+H^+$: 713.8560 [$M+H^+$]; found: 713.8563.

2-(16-(1-(7-(diethylamino)-2-oxo-2H-chromen-3-yl)-1H-1,2,3-triazol-4-yl)-2,3,5,6,8,9,11,12-octahydro-13H-benzo[*k*][1,4,7,10]tetraoxa[13]azacyclopentadecin-13-yl)methylacetate (4): Yield 38% (98 mg); M.p.: 163°C (decomp.); 1H NMR ($CDCl_3$, 300 MHz): δ = 8.70 (s, 1H), 8.41 (s, 1H), 7.45-7.33 (m, 3H), 6.98 (d, J = 7.5 Hz, 1H), 6.66 (d, J = 8.2 Hz, 1H), 6.54 (s, 1H), 4.26-3.53 (m, 21H), 3.48-3.39 (m, 4H), 1.22 ppm (t, J = 6.8 Hz, 6H); ^{13}C NMR ($CDCl_3$, 75 MHz): δ = 172.18, 156.89, 155.67, 151.73, 151.43, 147.47, 139.51, 134.32, 129.93, 124.25, 120.51, 119.63, 118.65, 116.86, 110.54, 110.00, 107.05, 96.91, 70.81, 70.63, 70.24, 70.10, 69.62, 68.99, 68.50, 53.48, 52.26, 51.52, 44.94, 12.38 ppm; HRMS (ESI): m/z calcd for $C_{32}H_{39}N_5O_8+H^+$: 622.2877 [$M+H^+$]; found: 622.2842.

7-(diethylamino)-3-(4-(2,3,5,6,8,9,11,12-octahydrobenzo[*b*][1,4,7,10,13]pentaoxacyclopentadecin-15-yl)-1H-1,2,3-triazol-1-yl)-2H-chromen-2-one (5): Yield 32% (73 mg); M.p.: 184°C (decomp.); 1H -NMR ($CDCl_3$, 300 MHz): δ = 8.72 (s, 1H), 8.42 (s, 1H), 7.53-7.35 (m, 3H), 6.92 (d, J = 8.3 Hz, 1H), 6.66 (dd, J = 8.9, 2.3 Hz, 1H), 6.54 (d, J = 2.1 Hz, 1H), 4.27-4.14 (m, 4H), 3.99-3.89 (m, 4H), 3.75 (s, 8H), 3.44 (q, J = 7.0 Hz, 4H), 1.22 ppm (t, J = 7.0 Hz, 6H); ^{13}C -NMR ($CDCl_3$, 75 MHz): δ = 156.91, 155.69, 151.45, 149.32, 149.11, 147.38, 134.35, 129.94, 123.81, 119.68, 118.77, 116.85, 114.05, 111.36, 110.03, 107.07, 96.94, 71.10, 71.07, 70.46, 70.43, 69.55, 69.51, 69.01, 68.93, 44.95, 12.38 ppm; HRMS (ESI): m/z calcd for $C_{29}H_{34}N_4O_7+H^+$: 551.2506 [$M+H^+$]; found: 551.2507.

10-(4-(4-(1,4,7,10-tetraoxa-13-azacyclopentadecan-13-yl)-3-methoxyphenyl)-1H-1,2,3-triazol-1-yl)-2,3,6,7-tetrahydro-1H,5H,11H-pyrano[2,3-*f*]pyrido[3,2,1-*i*]quinolin-11-one (8): Yield 20% (52 mg); M.p.: 126°C (decomp.); 1H NMR ($CDCl_3$, 300 MHz): δ = 8.72 (s, 1H), 8.32 (s, 1H), 7.47 (s, 1H), 7.38 (d, J = 7.7 Hz, 1H), 7.18 (d, J = 7.8 Hz, 1H), 6.99 (s, 1H), 3.94 (s, 3H), 3.80-3.33 (m, 20H), 3.32-3.28 (m, 4H), 2.90 (t, J = 6.4 Hz, 2H), 2.77 (t, J = 6.1 Hz, 2H), 2.02-1.92 ppm (m, 4H); ^{13}C NMR ($CDCl_3$, 75 MHz): δ = 157.04, 150.69, 147.19, 146.88, 134.65, 130.80, 125.84, 119.83, 119.72, 118.48, 118.40, 115.80, 115.39, 109.20, 109.10, 106.83, 106.06, 70.39, 70.18, 69.95, 69.88, 69.75, 55.65, 49.95, 49.53, 27.34, 21.02, 20.12, 20.08 ppm; HRMS (ESI): m/z calcd for $C_{34}H_{41}N_5O_7+H^+$: 632.3084 [$M+H^+$]; found: 632.3058.

3-(4-(4-(1,4,7,10-tetraoxa-13-azacyclopentadecan-13-yl)-3-methoxyphenyl)-1H-1,2,3-triazol-1-yl)-8-(dimethylamino)-2H-benzo[*g*]chromen-2-one (9): Yield 33% (86 mg); M.p.: 135°C (decomp.); 1H -NMR ($CDCl_3$, 300 MHz): δ = 8.78 (s, 1H), 8.58 (s, 1H), 7.94 (s, 1H), 7.83-7.75 (m, 1H), 7.50-7.32 (m, 3H), 7.24-7.21 (m, 1H), 7.13 (d, J = 8.9 Hz, 1H), 6.79 (s, 1H), 4.05-3.38 (m, 23H), 3.11 ppm (s, 6H); ^{13}C -NMR ($CDCl_3$, 125 MHz): δ = 156.57, 150.26, 149.86, 145.55, 137.40, 132.44, 129.85, 129.51, 123.87, 123.85, 120.35, 118.85, 118.62, 116.39, 113.18, 109.92, 109.50, 109.41, 109.30, 106.13, 103.95, 70.70, 70.50, 70.41, 70.31, 56.21, 55.77, 40.21 ppm; HRMS (ESI): m/z calcd for $C_{34}H_{39}N_5O_7+H^+$: 630.2928 [$M+H^+$]; found: 630.2917.

Keywords: sodium • potassium • fluorescence • fluorescent probes • crown compounds

- [1] a) E. Murphy, D. A. Eisner, *Circ. Res.* **2009**, *104*, 292-303; b) D. M. Bers, W. H. Barry, S. Despa, *Cardiovasc. Res.* **2003**, *57*, 897-912.
[2] A. Minta, R. Y. Tsien, *J. Biol. Chem.* **1989**, *264*, 19449-19457.

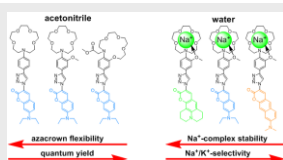
- [3] a) H. Szmazinski, J. R. Lakowicz, *Anal. Biochem.* **1997**, *250*, 131-138; b) A. P. de Silva, H. Q. N. Gunaratne, T. Gunnlaugsson, M. Nieuwenhuizen, *Chem. Commun.* **1996**, 1967-1968; c) M. K. Kim, C. S. Lim, J. T. Hong, J. H. Han, H.-Y. Jang, H. M. Kim, B. R. Cho, *Angew. Chem. Int. Ed.* **2010**, *49*, 364-367; d) A. R. Sarkar, C. H. Heo, M. Y. Park, H. W. Lee, H. M. Kim, *Chem. Commun.* **2014**, *50*, 1309-1312; e) M. Taki, H. Ogasawara, H. Osaki, A. Fukazawa, Y. Sato, K. Ogasawara, T. Higashiyama, S. Yamaguchi, *Chem. Commun.* **2015**, *51*, 11880-11883.
[4] a) H. He, M. A. Mortellaro, M. J. P. Leiner, S. T. Young, R. J. Fraatz, J. K. Tusa, *Anal. Chem.* **2003**, *75*, 549-555; b) T. Gunnlaugsson, M. Nieuwenhuizen, L. Richard, V. Thoss, *Tetrahedron Lett.* **2001**, *42*, 4725-4728.
[5] a) V. V. Martin, A. Rothe, K. R. Gee *Bioorg. Med. Chem. Lett.* **2005**, *15*, 1851-1855; b) V. V. Martin, A. Rothe, Z. Diwu, K. R. Gee *Bioorg. Med. Chem. Lett.* **2004**, *14*, 5313-5316; c) F. V. Englich, T. C. Foo, A. C. Richardson, H. Ebendorff-Heidepriem, C. J. Sumbly, T. M. Monro, *Sensors* **2011**, *11*, 9560-9572.
[6] a) P. Nandhikonda, M. P. Begaye, M. D. Heagy, *Tetrahedron Lett.* **2009**, *50*, 2459-2461; b) S. Uchiyama, E. Fukatsu, G. D. McClean, A. P. de Silva, *Angew. Chem.* **2016**, *128*, 778-781; *Angew. Chem. Int. Ed.* **2016**, *55*, 768-771.
[7] a) S. Ast, H. Müller, R. Flehr, T. Klamroth, B. Walz, H.-J. Holdt, *Chem. Commun.* **2011**, *47*, 4685-4687; b) S. Ast, T. Schwarze, H. Müller, A. Sukhanov, S. Michaelis, J. Wegener, O. S. Wolfbeis, T. Körzdörfer, A. Dürkop, H.-J. Holdt, *Chem. Eur. J.* **2013**, *19*, 14911-14917; c) T. Schwarze, J. Riemer, S. Eidner, H.-J. Holdt, *Chem. Eur. J.* **2015**, *21*, 11306-11310; d) T. Schwarze, R. Schneider, J. Riemer, H.-J. Holdt, *Chem. Asian J.* **2016**, *11*, 241-247.
[8] T. Schwarze, H. Müller, S. Ast, D. Steinbrück, S. Eidner, F. Geißler, M. U. Kumke, H.-J. Holdt, *Chem. Commun.* **2014**, *50*, 14167-14170.
[9] D. Kim, Q. P. Xuan, H. Moon, Y. W. Jun, K. H. Ahn, *Asian J. Org. Chem.* **2014**, *3*, 1089-1096.
[10] K. Sivakumar, F. Xie, B. M. Cash, S. Long, H. N. Barnhill, Q. Wang, *Org. Lett.* **2004**, *6* (24), 4603-4606.
[11] a) J. D. Lewis, J. N. Moore, *Dalton Trans.* **2004**, 1376-1385; b) L.-H. Lee, V. Lynch, R. J. Lagow, *J. Chem. Soc., Perkin Trans. 1* **2000**, 2805-2809.
[12] J. Pietruszka, A. Witt, *Synthesis* **2006**, *24*, 4266-4268.
[13] For the synthesis of 3-azido-8-(dimethylamino)-2H-benzo[*g*]chromen-2-one and for the determination of the K_d values see supporting information.
[14] a) V. V. Rostovtsev, L. G. Green, V. V. Folkin, K. B. Sharpless, *Angew. Chem. Int. Ed.* **2002**, *41*, 2596-2599; b) C. W. Tornøe, C. Christensen, M. Meldal, *J. Org. Chem.* **2002**, *67*, 3057-3062.
[15] D. Rehm, A. Weller, *Isr. J. Chem.* **1970**, *8*, 259-271.
[16] For **1**, **2** and **4** a reductive PET process from the ionophore to the fluorophore has different ΔG_{PET} values according to the Rehm-Weller equation $\Delta G_{PET} = E_{ox} - E_{red} - \Delta E_{00} - \Delta G_{ion\ pair}$.^[15] The oxidation potential E_{ox} of **1** is 0.75 V, of **2** is 0.77 V, of **4** is 0.80 V, of **5** is 1.30 V and of **7** is 1.37 V, respectively. The reduction potential of **1**, **2**, **4**, **5** and **7** E_{red} is -1.90 V ($Fc/Fc^+ = 0.09$ V in MeCN). In MeCN the ΔE_{00} for **1**, **2**, **4**, **5** and **7** is found at 448 nm ($\hat{=} 2.77$ eV). The ion-pairing energy $\Delta G_{ion\ pair}$ is ca. 0.1 eV under our conditions. Finally: ΔG_{PET} (**1**) = -0.22 eV, ΔG_{PET} (**2**) = -0.20 eV, ΔG_{PET} (**4**) = -0.17 eV, ΔG_{PET} (**5**) = +0.33 eV, ΔG_{PET} (**7**) = +0.39 eV.
[17] T. Lopez Arbeloa, F. Lopez Arbeloa, M. J. Tapia, I. Lopez Arbeloa, *J. Phys. Chem.* **1993**, *97*, 4704-4707.
[18] G. Jones II, M. A. Rahman, *J. Phy. Chem.* **1994**, *98*, 13028-13037.

For internal use, please do not delete. Submitted_Manuscript

Entry for the Table of Contents (Please choose one layout)

Layout 2:

FULL PAPER



Thomas Schwarze, Holger Müller, Darya Schmidt, Janine Riemer and Hans-Jürgen Holdt

Page No. – Page No.

Design of Na⁺-Selective Fluorescent Probes – A Systematic Study of the Na⁺-Complex Stability and the Na⁺/K⁺ Selectivity in Acetonitrile and Water

Herein, we report on the development of Na⁺-selective fluorescent probes, which containing of 15-membered crown ether ionophores and of coumarin or π -extended coumarin derivatives, as fluorophores. These fluoroionophores show different Na⁺-complex stabilities and Na⁺/K⁺ selectivities in acetonitrile and water.